

See discussions, stats, and author profiles for this publication at: <https://www.researchgate.net/publication/264381936>

Calculations of Mode-Specific Tunneling of Double-Hydrogen Transfer in Porphycene Agree with and Illuminate Experiment

ARTICLE in JOURNAL OF PHYSICAL CHEMISTRY LETTERS · JULY 2014

Impact Factor: 7.46 · DOI: 10.1021/jz501482v

CITATIONS

4

READS

41

3 AUTHORS:



Zahra Homayoon

Emory University

18 PUBLICATIONS 93 CITATIONS

SEE PROFILE



Joel M Bowman

Emory University

541 PUBLICATIONS 14,792 CITATIONS

SEE PROFILE



Francesco Evangelista

Emory University

31 PUBLICATIONS 1,051 CITATIONS

SEE PROFILE

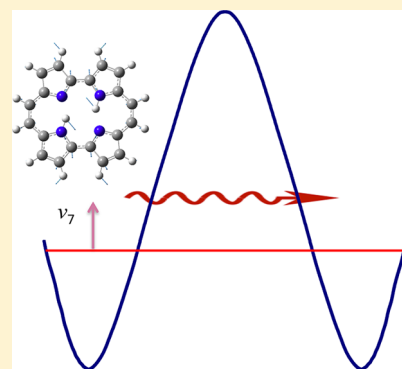
Calculations of Mode-Specific Tunneling of Double-Hydrogen Transfer in Porphycene Agree with and Illuminate Experiment

Zahra Homayoon,* Joel M. Bowman,* and Francesco A. Evangelista

Cherry L. Emerson Center for Scientific Computation and Department of Chemistry, Emory University, Atlanta, Georgia 30322, United States

S Supporting Information

ABSTRACT: We report a theoretical study of mode-specific tunneling splittings in double-hydrogen transfer in *trans*-porphycene. We use a novel, mode-specific “ Q_{im} path method”, in which the reaction coordinate is the imaginary-frequency normal mode of the saddle point separating the equivalent minima. The model considers all 108 normal modes and uses no adjustable parameters. The method gives the ground vibrational-state tunneling splitting, as well the increase in the splitting upon excitation of certain modes, in good agreement with experiment. Interpretation of these results is also transparent with this method. In addition, predictions are made for mode excitations not investigated experimentally. Results for d_1 and d_2 isotopologues are also in agreement with experiment.



SECTION: Spectroscopy, Photochemistry, and Excited States

Tunneling in chemical reactions is widely important as well as challenging, both experimentally and theoretically. Mode-specific tunneling is particularly challenging. It has recently been reported experimentally for symmetric H-atom transfer in malonaldehyde.¹ Full-dimensional (21 modes) quantum calculations of mode-specific tunneling in malonaldehyde have been done on an accurate potential energy surface.² This was a huge computational effort and is at the current state-of-the-art for such calculations.

Symmetric H-atom mode-specific tunneling has been reported for even larger molecules, for example, tropolone, dimers of 7-azaindole and 1-azacarbazole, and complexes of 7-hydroxyquinoline with ammonia or alcohol.^{3–10} Vibrationally assisted tunneling also has been proposed as the mechanism of enzyme-catalyzed reactions.^{11,12} The importance of this field has drawn significant attention experimentally and theoretically. Porphyrins, named “pigments of life”,¹³ are a class of hydrogen-bonded systems with two inner hydrogen atoms that can migrate between four nitrogen atoms and form the inner cavity and lead to chemically equivalent structures. Porphycene (PHC) (Figure 1) is a constitutional isomer of porphyrin with some significant characteristics that make it a potentially much better agent for photodynamic therapy than parent porphyrin and its derivatives.¹⁴ PHC is distinguished by the presence of strong N–H...N hydrogen bonds and by an extremely fast NH tautomerism. Recently, intramolecular double-hydrogen tunneling in *trans*-PHC has been the subject of several experimental studies^{14–17} using laser-induced fluorescence and dispersed fluorescence measured in supersonic jets. Doublet splitting of lines was observed; these disappear below experimental resolution upon double deuteration of the

inner nitrogen atoms. This finding was interpreted as an indication of double-hydrogen tunneling through a second-order saddle point (SP).¹⁴ One imaginary-frequency normal modes describes the symmetric double-H transfer in *trans*-PHC; that is the process of interest here. Later, enhanced tunneling splittings for several vibrational modes were reported in He nanodroplet experiments.¹⁷ The largest splitting increase was observed for fundamental excitation of vibrational mode 7, which involves symmetric motion of the N atoms. A qualitative explanation for enhancement of tunneling for this mode excitation was made,¹⁷ but no estimates of the tunneling splitting of this or any mode and the ground vibrational state were attempted. Approximate dynamical studies of concerted versus sequential H-atom transfer have also been reported^{18,19} but without a focus on the mode-specific tunneling splittings.

These experimental results of mode-specific tunneling in *trans*-PHC motivated us to undertake a theoretical study of these splittings. For a system this large, that is, 38 atoms and 108 normal modes, full-dimensional quantum calculations of the type mentioned above for malonaldehyde are not feasible. Even approximate approaches to mode-specific tunneling^{20–22} would not be feasible for a molecule this large. However, a recent approximate theory, based on the rectilinear, zero-curvature “ Q_{im} path”, applied successfully to mode-specific tunneling in malonaldehyde,²³ can be applied to these large systems and specifically for mode-specific tunneling of *trans*-

Received: July 15, 2014

Accepted: July 23, 2014

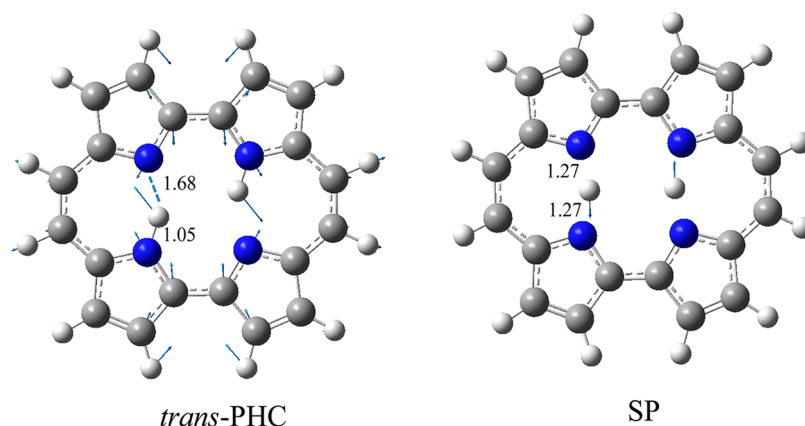


Figure 1. Structure of *trans*-PHC (and normal mode 7) and the SP (and the imaginary-frequency normal mode). N–H distances are given in Å.

PHC. This method was also used to describe the unimolecular dissociation of *cis*-HOCO to H + CO₂.²⁴ The theory was initially tested for ground-state tunneling splittings of a number of molecules and shown to be quite accurate. A summary of these comparisons is given in Table 1.

Table 1. Summary of Comparisons of Ground-State Tunneling Splittings (cm⁻¹) Using the Q_{im} Path against Benchmark, Full-Dimensional Quantum Calculations on the Same Potential Energy Surface

molecule	$V(Q_{\text{im}})$	benchmark
C ₂ H ₃ ^a	0.6	0.43
NH ₃ ^a	0.18	0.20
H ₃ O ^{++a}	19	22
malonaldehyde ^b	26	22
<i>d</i> ₁ -malonaldehyde ^b	4.6	3–4

^aReferences 26 and 30. ^bReference 31.

In brief, the theory is as follows. First, the Q_{im} path is the displacement of the imaginary-frequency normal mode of the SP separating the two wells. Then, at each value of Q_{im} , the full potential is minimized; the resulting potential is denoted $V(Q_{\text{im}})$. The central component of the mode-specific theory is the projection of the normal modes of a minimum onto the Q_{im} path. The effect of mode excitation is mapped onto the change of the turning points on $V(Q_{\text{im}})$, and the resulting change in tunneling probability is then easily calculated, semiclassically. The tunneling splitting is given by the well-known semiclassical expression

$$\Delta = \frac{\hbar\omega}{\sqrt{e\pi}} e^{-\theta} \quad (1)$$

$$\theta = \frac{1}{\hbar} \int_{a_1}^{a_2} dQ_{\text{im}} \sqrt{2(V(Q_{\text{im}}) - E)} \quad (2)$$

where ω is the harmonic frequency at the minimum of $V(Q_{\text{im}})$ and a_1 and a_2 are the classical turning points. To determine how the excitation of mode i of the “reactant” molecule changes the turning point, the projection model is introduced to relate the change in Q_{im} to the displacement of normal mode i of the minimum, Q_i , in quantum state n_i . The change in turning points in Q_{im} upon excitation of mode i relative to the ground state is given by,²³

$$\Delta Q_{\text{im}}^{\text{tp}}(n_i) = |q_{\text{im}}^{\text{T}} q_i| (|Q_i^{\text{tp}}(n_i)| - |Q_i^{\text{tp}}(n_i = 0)|) \quad (3)$$

where $|q_{\text{im}}^{\text{T}} q_i|$ is the projection of the unit vectors of the mass-scaled, imaginary-frequency normal mode of the SP and analogous normal mode i of the molecule and where the turning points of mode i are given by $Q_i^{\text{tp}} = \pm[(2n_i + 1)/\omega_i]^{1/2}$, where ω_i is the corresponding harmonic frequency. We have chosen the sign to conform to the choice of the left well as the minimum; therefore, the change $\Delta Q_{\text{im}}^{\text{tp}}$ is positive. A positive change results in a decrease in θ and thus an increase in the splitting. E in eq 2 is the value of $V(Q_{\text{im}})$ at the changed turning points. From the above, it is clear that this theory requires only $V(Q_{\text{im}})$ and normal-modes analyses of the SP and one minimum (in the potential of a symmetry double well). Therefore, this method can be applied for large molecules.

The first step in applying this theory is the calculation of the relaxed potential as a function of the mass-scaled, rectilinear, imaginary-frequency normal mode of the relevant SP that connects the minima. This step was carried out by performing a calculation of the intrinsic reaction path (IRC) in mass-scaled Cartesian coordinates and then making the linear transformation to Q_{im} at each point along the IRC. We verified that the IRC connects the SP to the minima of interest, in this case, the symmetric forms of *trans*-PHC.

The optimization of the stationary, normal-mode analyses and IRC calculations mode was accomplished using the DFT-B3LYP/6-31G(d,p) level of theory, as implemented in Gaussian 09.²⁵ From the IRC, the Q_{im} path was determined. The structures of the minimum and SP and also normal mode 7 of the minimum and the double-H transfer of the imaginary-frequency normal mode are shown in Figure 1. The barrier obtained with this method is 6.4 kcal/mol, and calculations of tunneling splitting were initially done with this $V(Q_{\text{im}})$, and some results of those calculations will be discussed below. In short though, agreement with experiment is very good using this potential. We also performed a calculation of the barrier height, using the DFT minimum and SP configurations, with the coupled cluster singles and doubles with perturbative triples [CCSD(T)] theory with the cc-pVDZ basis.³² This was a very CPU and memory intensive calculation and yielded a barrier of 6.8 kcal/mol.

Conventional CCSD(T) calculations using a larger basis are not feasible for us, and therefore, CCSD(T) calculations were done using the domain-based local pair natural orbital approximation (DLPNO)^{33,34} as implemented in the quantum chemistry package Orca.³⁵ Details of these calculations are as follows. Correlation-consistent basis sets of Dunning (cc-pVXZ, where X = D,T,Q)³² were used, and complete basis results were

obtained by extrapolation according to the focal point method.³⁶ The Hartree–Fock energy was fitted to the function $A + B \exp(-CX)$ using the points $X = 2, 3$, and 4 .³⁷ The DLPNO-CCSD(T) correlation energy was instead fitted to the function $A + BX^{-3}$ using the points $X = 2$ and 3 .³⁸ Results are given in Table 2. (Note that the barrier using this method and

Table 2. Indicated Calculations of the Barrier Height (ΔE , in kcal/mol) for Double-H Transfer of *trans*-PHC

basis set	method		ΔE total
	HF	$\Delta\text{CCSD(T)}^a$	
cc-pVDZ	14.77	−7.81	6.96
cc-pVTZ	15.80	−7.72	8.08
cc-pVQZ	15.96		
complete	15.97	−7.68	8.28

^a $\Delta\text{CCSD(T)}$ denotes the CCSD(T) correlation energy.

the cc-pVDZ basis is only 0.19 kcal/mol higher than the one obtained with conventional CCSD(T)/cc-pVDZ.) Several points along the Q_{im} path were computed at the DLPNO-CCSD(T) level of theory using the cc-pVTZ basis set.

These data, specifically the cc-pVTZ ones, were used to modify the $V(Q_{\text{im}})$ obtained with DFT-B3LYP/6-31G(d,p) calculations. Basically, a simple multiplicative scaling was done to obtain the potential shown in Figure 2. As seen, the barrier

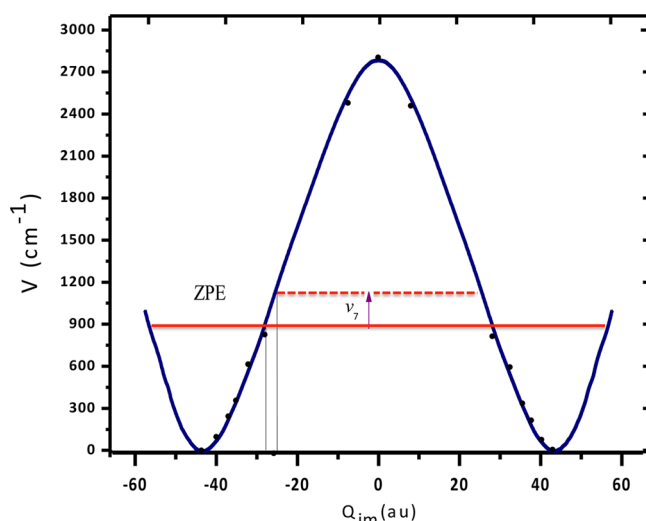


Figure 2. Potential along the mass-scaled Q_{im} path of *trans*-PHC (blue curve) and turning points relevant to a tunneling integral indicated for the zero-point state and for excitation of mode 7. The filled circles are the energies obtained from DLPNO-CCSD(T)/cc-pVTZ calculations, described in the text.

height is 2826 cm^{-1} (8.08 kcal/mol), and at the minima, $|Q_{\text{im}}|$ equals 43.0. Also as seen, the modified potential reproduces the additional DLPNO-CCSD(T) cc-pVTZ energies very well. The harmonic frequency was determined from a fit to $V(Q_{\text{im}})$ from several points starting at the minimum. Then, the relevant turning points for the ground state, indicated in the figure, were determined from the harmonic zero-point energy. The change in these turning points upon excitation of mode 7 is also indicated, and the details of the determination of these are given next.

To determine the change in turning points upon excitation of the modes of *trans*-PHC, given by eq 3, a normal-mode analysis

of the double-H-atom SP and the *trans*-PHC minimum was done, as noted above, using DFT-B3LYP/6-31G(d,p). The normal-mode frequencies and symmetries of *trans*-PHC are given in Table S1 of the Supporting Information (SI). Comparison with experiment¹⁷ shows good agreement, especially for mode 7, indicating that the harmonic description of that mode is reasonable. Note, the SP is second-order, and Figure S1 of the SI shows the two imaginary-frequency normal modes. As seen there, the imaginary-frequency mode of b_{3g} symmetry ($i 1206 \text{ cm}^{-1}$) is the one that described the double-H transfer of *trans*-PHC, in agreement with a previous instanton analysis¹⁸ and from an insightful 2D analysis for porphine.²⁷ Next, we calculated the projections $|q_{\text{im}}^T q_i|$. These are also given in Table S1 of the SI, where, as seen, most modes have zero projection.

We begin by investigating splittings for the ground state and also those modes reported experimentally. Table 3 gives

Table 3. Splittings (cm^{-1}) and ΔQ_{im} for the Ground State and Mode Excitation of *trans*-PHC from Projection Theory and Experiment

mode	ΔQ_{im}	theory	experiment ^a
ground state	0.0	4.1	4.43
ν_7	3.3	10.1	12
$\nu_7 + \nu_{15}$	4.0	11.7	12.4
$\nu_7 + \nu_{16}$	3.6	11.0	12.1
ν_{15}	0.77	5.4	4.6
ν_{16}	0.43	4.9	4.6
$2\nu_{15}$	1.3	6.3	5
$\nu_{15} + \nu_{16}$	1.17	6.1	4.9

^aReference 17.

calculated and experimental splittings. As seen, the calculated ground-state splitting of 4.3 cm^{-1} is in excellent agreement with the experimental value of 4.43 cm^{-1} . Experimentally, the largest splitting for double-hydrogen tunneling of *trans*-PHC is for ν_7 and is equal to 12 cm^{-1} . The projection theory predicts a splitting of 10.1 cm^{-1} for this mode. For the combination states $\nu_7 + \nu_{15}$ and $\nu_7 + \nu_{16}$, 12.4 and 12.1 cm^{-1} splittings were reported,¹⁷ and the present theory gives 11.7 and 11.0 cm^{-1} , respectively, for these states. For ν_{15} , ν_{16} , $2\nu_{15}$, and $\nu_{15} + \nu_{16}$, we see no strong differences in splitting, in good agreement with experiment, as seen in Table 3. These splittings correlate, as expected, with the change in the classical turning points, which are also given in Table 3. Mode 7 in particular has the largest change in turning point, and this is due in part to its low vibrational frequency (186 cm^{-1}). Note that this also implies that this mode can easily be activated thermally, and therefore, a significant increase in tunneling with temperature is predicted. Several other modes that have large projections are seen in Table S1 (SI). The largest ones are high-frequency N–H stretch modes 95 and 96. Splittings of 15 and 12 cm^{-1} are predicted for these modes. No experimental results are available to compare with them. Before considering the effect of deuteration, we note that the projection $|q_{\text{im}}^T q_i|$, which results from simply relating two sets of mass-scaled normal-mode displacements,²³ has been used extensively and successfully by Guo and co-workers to qualitatively correlate vibrational and/or rotational excitation of reactants to enhancement in reactivity in bimolecular reactions.²⁸ Similarly and independently, it was used by Siebrand and co-workers to qualitatively

rationalize the effects of mode-specific tunneling in malonaldehyde.²⁹

The effect of deuteration on tunneling has been reported experimentally. In order to investigate this theoretically, we calculated the Q_{im} path of singly deuterated (*trans*-PHC- d_1) and doubly deuterated *trans*-PHC (*trans*-PHC- d_2). From normal-mode analysis, we calculate the imaginary frequency of double-H transfer of *trans*-PHC- d_1 and *trans*-PHC- d_2 as i 1150 and i 869, respectively. Harmonic frequencies of *trans*-PHC- d_1 and *trans*-PHC- d_2 and projection values of modes into imaginary modes of SPs are given on Tables S2 and S3 of the SI. Figure 3

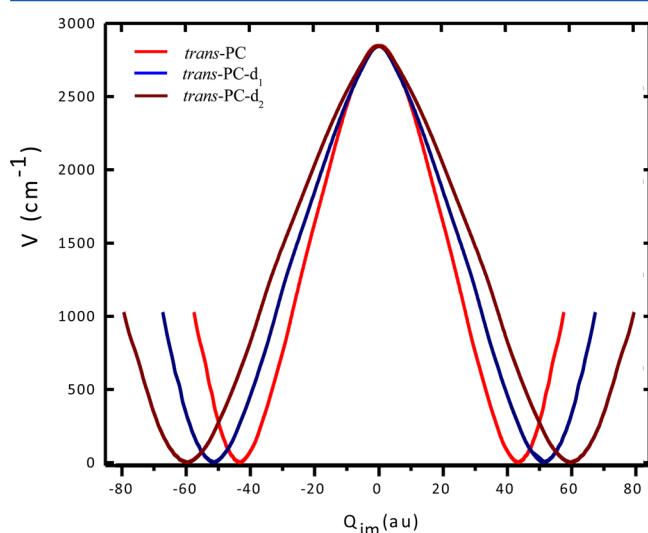


Figure 3. Potential along the mass-scaled Q_{im} path of *trans*-PHC, *trans*-PHC- d_1 , and *trans*-PHC- d_2 .

shows the Q_{im} pathways of *trans*-PHC- d_1 and *trans*-PHC- d_2 . These pathways again were calculated using the IRC. Deuteration affects the Q_{im} pathway by widening the potential and also by decreasing the zero-point energy; both effects lead to a decrease of tunneling splitting. For *trans*-PHC- d_1 and *trans*-PHC- d_2 minima, $|Q_{\text{im}}|$ equal 51.0 and 59.0 atomic units, respectively. The calculated splittings of the ground state and mode excitation of *trans*-PHC- d_1 are given in Table 4. The

Table 4. Splittings (cm^{-1}) for the Ground State and Mode Excitation of *trans*-PHC- d_1 from Theory and Experiment

mode	theory	experiment ^a
ground state	0.87	0.58
ν_7	1.8	2.3
$\nu_7 + \nu_{15}$	2.1	2.4
$\nu_7 + \nu_{16}$	1.9	2.4

^aReference 17.

calculated ground-state splitting of *trans*-PHC- d_1 is 0.87 cm^{-1} , in good agreement with experiment. Again, ν_7 plays an important role in enhancement of tunneling, as seen in Table 4. For *trans*-PHC- d_2 , the calculated ground-state splitting is 0.05 cm^{-1} , which is too small to be resolved in the experiments, which reported no splitting.

Finally, we comment on the robustness of the present results. As noted above, calculations were also done using the $V(Q_{\text{im}})$ potential directly from DFT-B3LYP/6-31G(d,p) calculations. The barrier height of this potential is 6.4 kcal/mol , which is

roughly 20% lower than the more accurate DLPNO-CCSD-(T)/cc-pVTZ barrier used in the calculations that we just reported. The resulting tunneling splittings using the lower-barrier $V(Q_{\text{im}})$ are almost uniformly 20% larger than the ones reported in Tables 3 and 4. Given the nonlinear nature of the tunneling integral, this 20% increase may seem surprising at first glance. However, the major reason for this is the decrease in the ZPE of the lower-barrier $V(Q_{\text{im}})$, and thus, the classical turning points also change in a manner that partially compensates for the decrease in the action θ . Thus, we have confidence that the present results, which are based on a very simple theory, are well within the 20% quantitative accuracy that was noted in the discussion of Table 1.

In summary, application of the harmonic projection theory to *trans*-PHC and its singly and doubly deuterated isotopologues gives tunneling splittings in very good agreement with experiment and provides a simple explanation of the experimental results. This level of agreement is within the expected level of accuracy of 10–20% based on previous tests of the theory against benchmark results.

■ ASSOCIATED CONTENT

■ Supporting Information

A comparison of tunneling splittings against exact benchmark results, several normal modes of SP and *trans*-PHC, tables of normal-mode analysis, and projection of the imaginary mode of the SP and *trans*-PHC, *trans*-PHC- d_1 , and *trans*-PHC- d_2 . This material is available free of charge via the Internet at <http://pubs.acs.org>.

■ AUTHOR INFORMATION

Corresponding Authors

*Email: zhomayo@emory.edu (Z.H.).

*E-mail: jmbowma@emory.edu (J.M.B.).

Notes

The authors declare no competing financial interest.

■ ACKNOWLEDGMENTS

Z.H. and J.M.B. thank the Army Research Office (W911NF-11-1-0477) for financial support.

■ REFERENCES

- (1) Lüttschwager, N. O. B.; Wassermann, T. N. S.; Coussan; Suhm, M. A. Vibrational tuning of the hydrogen transfer in malonaldehyde — A combined FTIR and Raman jet study. *Mol. Phys.* **2013**, *111*, 2211–2227.
- (2) Hammer, T.; Manthe, U. Iterative diagonalization in the state-averaged multi-configurational time-dependent Hartree approach: Excited state tunneling splittings in malonaldehyde. *J. Chem. Phys.* **2012**, *136*, 054105/1–052105/17.
- (3) Sekiya, H.; Nagashima, Y.; Nishimura, Y. Electronic spectra of jet-cooled tropolone. Effect of the vibrational excitation on the proton tunneling dynamics. *J. Chem. Phys.* **1990**, *92*, 5761–5769.
- (4) Sekiya, H.; Nagashima, Y.; Tsuji, T.; Nishimura, Y.; Mori, A.; Takeshita, H. Vibrational mode-specific tunneling splittings in the A states of deuterated tropolones. *J. Phys. Chem.* **1991**, *95*, 10311–10317.
- (5) Fuke, K.; Kaya, K. Dynamics of double-proton-transfer reaction in the excited-state model hydrogen-bonded base pairs. *J. Phys. Chem.* **1989**, *93*, 614–621.
- (6) Sakota, K.; Okabe, C.; Nishi, N.; Sekiya, H. Excited-State double-proton transfer in the 7-azaindole dimer in the gas phase. 3. Reaction mechanism studied by picosecond time-resolved REMPI spectroscopy. *J. Phys. Chem. A* **2005**, *109*, 5245–5247.

- (7) Tanner, C.; Manca, C.; Leutwyler, S. Probing the threshold to H atom transfer along a hydrogen-bonded ammonia wire. *Science* **2003**, 302, 1736–1739.
- (8) Manca, C.; Tanner, C.; Coussan, S.; Leutwyler, S. H atom transfer along an ammonia chain: Tunneling and mode selectivity in 7-hydroxyquinoline (NH_3)₃. *J. Chem. Phys.* **2004**, 121, 2578–2590.
- (9) Tanner, C.; Manca, C.; Leutwyler, S. Exploring excited-state hydrogen atom transfer along an ammonia wire cluster: Competitive reaction paths and vibrational mode selectivity. *J. Chem. Phys.* **2005**, 122, 204326/1–204326/11.
- (10) Kwon, O. H.; Lee, Y. S.; Yoo, B. K.; Jang, D. Excited-state triple proton transfer of 7-hydroxyquinoline along a hydrogen-bonded alcohol chain: Vibrationally assisted proton tunneling. *J. Angew. Chem., Int. Ed.* **2006**, 45, 415–419.
- (11) Knapp, M. J.; Klinman, J. P. Environmentally coupled hydrogen tunneling. Linking catalysis to dynamics. *Eur. J. Biochem.* **2002**, 269, 3113–3121.
- (12) Sutcliffe, M. J.; Scrutton, N. S. A new conceptual framework for enzyme catalysis. Hydrogen tunnelling coupled to enzyme dynamics in flavoprotein and quinoprotein enzymes. *Eur. J. Biochem.* **2002**, 269, 3096–3102.
- (13) Battersby, A. R.; Fookes, C. J. R.; Matcham, G. W. J.; McDonald, E. Biosynthesis of the pigments of life: formation of the macrocycle. *Nature* **1980**, 285, 17–21.
- (14) Vdovin, A.; Sepiół, J.; Urbanska, N.; Pietraszkiewicz, M.; Mordzinski, A.; Waluk, J. Evidence for two forms, double hydrogen tunneling, and proximity of excited states in bridge-substituted porphycenes: Supersonic jet studies. *J. Am. Chem. Soc.* **2006**, 128, 2577–2586.
- (15) Waluk, J. Ground- and excited-state tautomerism in porphycenes. *Acc. Chem. Res.* **2006**, 39, 945–951.
- (16) Gil, M.; Waluk, J. Vibrational gating of double hydrogen tunneling in porphycene. *J. Am. Chem. Soc.* **2007**, 129, 1335–1341.
- (17) Vdovin, A.; Waluk, J.; Dick, B.; Slenczka, A. Mode-selective promotion and isotope effects of concerted double-hydrogen tunneling in porphycene embedded in superfluid helium nanodroplets. *ChemPhysChem* **2009**, 10, 761–765.
- (18) Smedarchina, Z.; Shibl, M. F.; Kuhn, O.; Fernandez-Ramos, A. The tautomerization dynamics of porphycene and its isotopomers — Concerted versus stepwise mechanisms. *Chem. Phys. Lett.* **2007**, 436, 314–321.
- (19) Walewski, L.; Waluk, J.; Lesyng, B. Car–Parrinello molecular dynamics study of the intramolecular vibrational mode-sensitive double proton-transfer mechanisms in porphycene. *J. Phys. Chem. A* **2010**, 114, 2313–2318.
- (20) Makri, N.; Miller, W. A semiclassical tunneling model for use in classical trajectory simulations. *J. Chem. Phys.* **1989**, 91, 4026–4036.
- (21) Barnes, G. L.; Squires, S. M.; Sibert, E. L., III. Symmetric double proton tunneling in Formic Acid dimer: A diabatic basis approach. *J. Phys. Chem. B* **2008**, 112, 595–603.
- (22) Nakamura, H.; Mil'nikov, G. *Quantum mechanical tunneling in chemical physics*; CRC: Boca Raton, FL, 2013.
- (23) Wang, Y.; Bowman, J. M. Mode-specific tunneling using the Q_{im} path: Theory and an application to full-dimensional malonaldehyde. *J. Chem. Phys.* **2013**, 139, 154303/1–154303/5.
- (24) Wang, X.; Bowman, J. M. Mode-specific tunneling in the unimolecular dissociation of *cis*-HOCO to H + CO₂. *J. Phys. Chem. A* **2014**, 118, 684–689.
- (25) Frisch, M. J.; Trucks, G. W.; Schlegel, H. B.; Scuseria, G. E.; Robb, M. A.; Cheeseman, J. R.; Scalmani, G.; Barone, V.; Mennucci, B.; Petersson, G. A.; et al. *Gaussian 09*, revision C.01; Gaussian, Inc.: Wallingford, CT, 2010.
- (26) Wang, Y.; Braams, B. J.; Bowman, J. M.; Carter, S.; Tew, D. P. Full-dimensional quantum calculations of ground-state tunneling splitting of malonaldehyde using an accurate *ab initio* potential energy surface. *J. Chem. Phys.* **2008**, 128, 224314/1–224314/21.
- (27) Smedarchina, Z.; Siebrand, W. Correlated double-proton transfer. I. Theory. *J. Chem. Phys.* **2007**, 127, 174513/1–174513/12.
- (28) Jiang, B.; Guo, H. Hybrid models of molecular machines and the no-pumping theorem. *J. Chem. Phys.* **2013**, 138, 234104/1–234104/10.
- (29) Siebrand, W.; Smedarchina, Z.; Fernandez-Ramos, A. Selection rules for tunneling splitting of vibrationally excited levels. *J. Chem. Phys.* **2013**, 139, 021101/1–021101/4.
- (30) Kamarchik, E.; Wang, Y.; Bowman, J. M. Reduced-dimensional quantum approach to tunneling splittings using saddle-point normal coordinates. *J. Phys. Chem. A* **2009**, 113, 7556–7562.
- (31) Wang, Y.; Bowman, J. M. One-dimensional tunneling calculations in the imaginary-frequency, rectilinear saddle-point normal mode. *J. Chem. Phys.* **2008**, 129, 121103/1–121103/4.
- (32) Dunning, T. H., Jr. Gaussian basis sets for use in correlated molecular calculations. I. The atoms boron through neon and hydrogen. *J. Chem. Phys.* **1989**, 90, 1007–1023.
- (33) Riplinger, C.; Neese, F. An efficient and near linear scaling pair natural orbital based local coupled cluster method. *J. Chem. Phys.* **2013**, 138, 034106.
- (34) Riplinger, C.; Sandhoefer, B.; Hansen, A.; Neese, F. Natural triple excitations in local coupled cluster calculations with pair natural orbital. *J. Chem. Phys.* **2013**, 139, 134101.
- (35) Neese, F. The ORCA program system. *Wiley Interdiscip. Rev.: Comput. Mol. Sci.* **2012**, 2, 73–78.
- (36) East, A.; Allen, W. D. The heat of formation of NCO. *J. Chem. Phys.* **1993**, 99, 4638–4650.
- (37) Feller, D. The use of systematic sequences of wave functions for estimating the complete basis set, full configuration interaction limit in water. *J. Chem. Phys.* **1993**, 98, 7059–7071.
- (38) Helgaker, T.; Klopper, W.; Koch, H.; Noga, J. Basis-set convergence of correlated calculations on water. *J. Chem. Phys.* **1997**, 106, 9639–9646.